Bioanalytical Methods

DOI: 10.1002/anie.200804518

SERS Labels for Red Laser Excitation: Silica-Encapsulated SAMs on Tunable Gold/Silver Nanoshells**

*Bernd Küstner, Magdalena Gellner, Max Schütz, Friedrich Schöppler, Alexander Marx, Philipp Ströbel, Patrick Adam, Carsten Schmuck, and Sebastian Schlücker**

The interaction of functional nanomaterials with biomolecules is a central topic in nanobiotechnology.[1] Detection, labeling, and sensing of biomolecules are just a few examples of applications.[2] Surface-enhanced Raman scattering (SERS), an ultrasensitive technique of Raman spectroscopy for molecules near metallic nanostructures, plays an increasingly important role in this research area.[3] In comparison with established labeling approaches such as molecular fluorophores, SERS-based detection schemes offer several unique advantages. A very important benefit is the tremendous multiplexing capacity of SERS: the enormous potential for the parallel detection of numerous target molecules with SERS labels is a result of the small linewidth of vibrational Raman bands.[4] From a practical point of view, simultaneous excitation of the characteristic spectral signatures from various distinct Raman labels requires only a single laser wavelength. Additional important aspects are the quantification of target molecule concentration and the extreme sensitivity of SERS, particularly SERRS (surface-enhanced resonance Raman scattering).[5]

Various nanoparticle probes for the detection of proteins[6] and nucleic acids[7] by SERS/SERRS are already available. One major difference in their designs is that they are based either on a self-assembled monolayer (SAM) of Raman label molecules on the nanoparticle surface or on the encapsulation of a submonolayer of Raman labels. An encapsulated SAM, i.e., the combination of both important features, however, has not been reported so far.

The presence of a SAM on the nanoparticle surface has several key benefits. For example, coadsorption of molecules other than Raman labels is eliminated or at least minimized, thereby avoiding interference with unwanted spectral contributions. Additionally, a SAM ensures maximum coverage of the nanoparticle surface with Raman reporter molecules, thereby providing maximum SERS sensitivity for a given Raman label. Spectroscopically, the uniform orientation of the reporter molecules relative to the surface normal of the nanoparticle leads to narrow and reproducible Raman bands from only a small number of normal modes (SERS selection rules[3a]). These properties are all extremely important in terms of multiplexing. Particle aggregation and desorption of Raman label molecules from the nanoparticle surface are two major drawbacks of this concept because the SAM and the solvent environment are in direct contact. Encapsulation, however, would eliminate or at least minimize these disadvantages, resulting in both chemical and mechanical stability. A protective shell can be accomplished with different materials such as silica and polymers including proteins.[1,2] In particular silica is attractive because of its potential for long-term storage of the SERS labels. Earlier designs for silica-encapsulated SERS labels were based on the coadsorption of Raman reporter molecules together with SiO_2 precursors on the nanoparticle surface.[8] However, this approach does not provide a complete and densely packed SAM, with the advantages discussed above.

We report here, for the first time, the silica encapsulation of a SAM on metallic nanoparticles (Figure 1). In this approach the advantages of both the SAM and the silica shell are integrated into a single functional unit. Using a SAM on gold/silver nanoshells, which are optimized for red laser excitation, we find that our SERS labels for bioanalytical

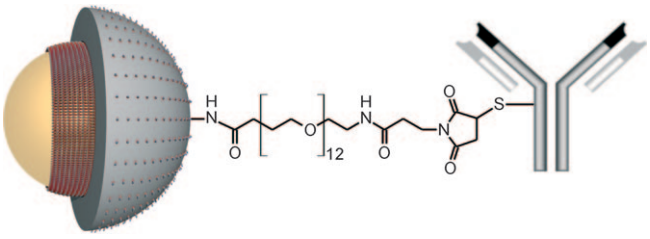

Figure 1. Structure of silica-encapsulated and biofunctionalized SERS labels. Left: Gold/silver nanoparticle with a SAM of Raman label molecules (red) and a protective silica shell with amino groups (gray). Middle: heterobifunctional polyethylene glycol spacer. Right: monoclonal antibody for antigen recognition.

[*] B. Küstner, M. Gellner, M. Schütz, F. Schöppler, Prof. Dr. S. Schlücker
Institut für Physikalische Chemie, Universität Würzburg
Am Hubland, 97074 Würzburg (Germany)
E-mail: sebastian.schluecker@uos.de
Prof. Dr. A. Marx, Prof. Dr. P. Ströbel
Institut für Pathologie, Universitätsklinikum Mannheim
Theodor-Kutzer-Ufer 1–3, 68167 Mannheim (Germany)
Dr. P. Adam
Institut für Pathologie, Universität Würzburg
Josef-Schneider-Strasse 2, 97080 Würzburg (Germany)
Prof. Dr. C. Schmuck
Institut für Organische Chemie, Universität Duisburg-Essen
Universitätsstrasse 5, 45141 Essen (Germany)

[**] Financial support from the German Research Foundation (DFG; SCHL 594/4-1 and Heisenberg fellowship for S.S.), the German Federal Ministry of Science and Education (BMBF; EXIST Seed; B.K., M.S., and S.S.), Freistaat Bayern (FLÜGGE; M.G. and M.S.), and the Center for Clinical Research at the University of Würzburg (A.M., P.S., and P.A.) is acknowledged. We thank Florian Baum, Oliver Breunig, Timo Hefner, Carina Jehn, Kristin Kröker, Nicolas Rühl, and Sandra Sänze for technical support. SERS: surface-enhanced Raman scattering, SAM: self-assembled monolayer.

Supporting information for this article is available on the WWW under http://dx.doi.org/10.1002/anie.200804518.

applications give signals approximately 180 times more intense than those of other labels based on single gold particles. SERS mapping experiments combined with scanning electron microscopy (SEM) document reproducible SERS signals on a particle-to-particle basis. Finally, the application of these improved nanoparticle probes in SERS microscopy[9] for selective imaging of a target protein in a prostate tissue sample is demonstrated.

Our approach to SERS labels for biomedical applications presented here (Figure 1) is based on single colloidal gold/silver nanoshells with tunable plasmon resonances in the red to near-infrared region.[10,11] This is important because long-wavelength laser excitation minimizes cellular or tissue autofluorescence, which degrades the signal-to-background ratio and image contrast. In particular, it is important for applications in vivo.[12] The gold/silver nanoshells form the SERS substrate, which is completely covered with an organic SAM of Raman labels.[9b,11a] The outermost shell of silica has not only a protective function, but it also allows efficient bioconjugation.[13] Nanoparticle encapsulation and functionalization are therefore essential for obtaining the required selectivity, sensitivity, and stability.

Gold/silver nanoshells were prepared according to procedures published by Xia and co-workers.[10] The average diameter is about 60 nm, the shell thickness is about 5 nm (Figure 2). Silica encapsulation for SAM protection and

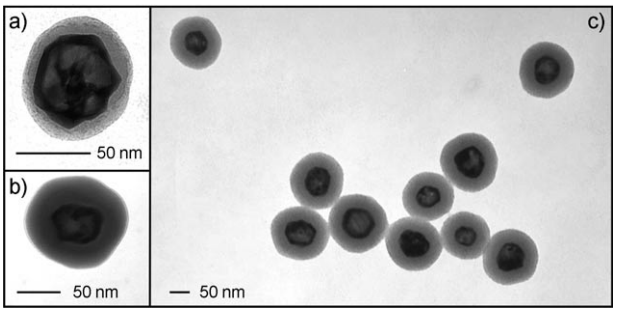

Figure 2. TEM images of silica-encapsulated SERS labels with silica shells ≈10 nm (a) and ≈25 nm (b, c) thick. The diameter of the gold/silver nanoshells is ≈60 nm.

further biofunctionalization was achieved by coating the SAM with a polyelectrolyte (layer-by-layer deposition) and then growing the silica shell by a modified Stöber method.[14] In this polyelectrolyte method, the SAM is first covered with poly(allylamine hydrochloride) and then coated with polyvinylpyrrolidone. Growth of the silica shell is achieved by using an ammonia/2-propanol mixture and tetraethylorthosilicate (TEOS) in 2-propanol. The TEM pictures of the silica-encapsulated gold/silver nanoshells in Figure 2 document the high reproducibility of this method. In Figure 2a, the gold/silver nanoshell is covered with a silica shell roughly 10 nm thick. A thicker silica shell (≈25 nm) is obtained by increasing the amount of TEOS (Figure 2b, c).

In order to demonstrate that the nanoshells give reproducible SERS signals on a particle-to-particle basis, we performed a combined SERS/SEM experiment (Figure 3). The

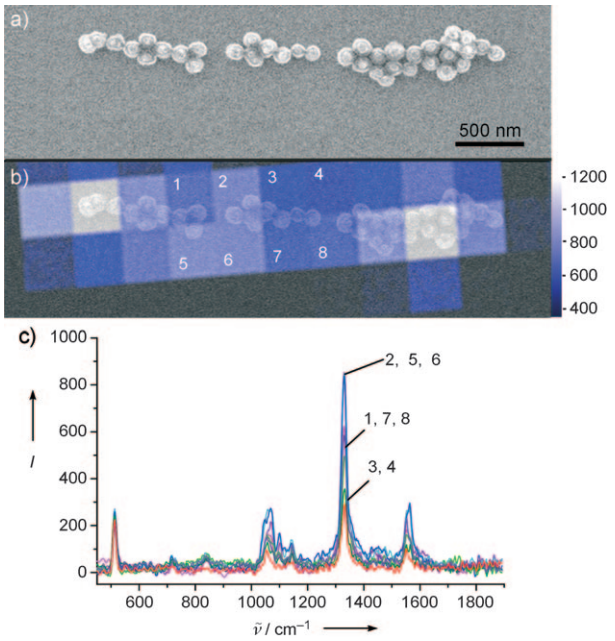

Figure 3. a) Scanning electron microscopy (SEM) image of silica-encapsulated SERS labels on a silicon wafer. b) False-color SERS map overlaid with the SEM image. c) SERS spectra obtained from squares labeled 1–8 in (b). The Raman label precursor molecule is 5,5′-dithiobis(2-nitrobenzoic acid).

SEM image (Figure 3a) shows that the majority of particles are monomers and that only a small fraction (15–16%) are encapsulated dimers. The overlaid false-color SERS image was obtained in a Raman mapping experiment on the same particles (Figure 3b). The bright pixels indicate that the few dimers have a high signal strength. The corresponding SERS spectra (Figure 3c) demonstrate that the SERS signals are reproducible. The Raman label precursor was 5,5′-dithiobis(2-nitrobenzoic acid), which exhibits dominant SERS bands at roughly 1340 cm^{-1} (symmetric NO_2 stretch), and at 1050 and 1550 cm^{-1} (phenyl ring modes).

The presence of a SAM on a SERS substrate has several important implications. One aspect is the number of bands observed in the corresponding spectra. Figure 4 shows a comparison between 4-mercaptobenzoic acid (4-MBA) as a SAM and rhodamine 6G (R6G) on gold/silver nanoshells. It is obvious that the presence of a SAM is beneficial in terms of multiplexing: the SERS spectrum of 4-MBA (Figure 4a) exhibits only two dominant SERS bands at 1082 and 1592 cm^{-1}, while many more peaks are observed in the R6G spectrum (Figure 4b).

The signal strength of the SERS labels is a further very important aspect. Here, the advantages of a complete SAM comprising only Raman label molecules is most evident: it provides the maximum surface coverage and therefore the highest possible sensitivity. In Figure 5a the higher sensitivity of a complete SAM compared with that of a submonolayer coverage of Raman labels, both on the same SERS substrate, is evident. Colloidal solutions of gold/silver nanoshells were incubated with a) 4-MBA and b) a 1:9 mixture of 4-MBA and 3-mercapto-*n*-propyltrimethoxysilane (MPTMS), both in eth-

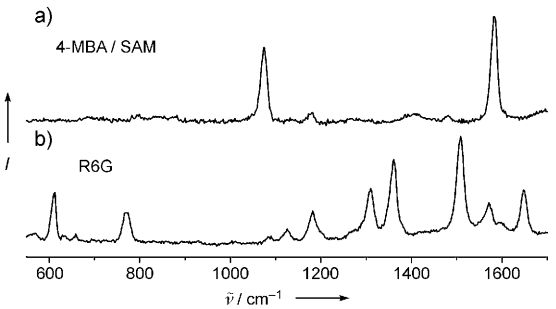

Figure 4. a) The SERS spectrum of 4-mercaptobenzoic acid present as a SAM on gold/silver nanoshells exhibits only two dominant Raman bands. b) In contrast, the SERS spectrum of rhodamine 6G exhibits many bands. Both spectra were obtained with red laser excitation ($\lambda = 632.8$ nm).

anol/polyvinylpyrrolidone. This and other stoichiometries (1:20) were used in prior approaches for silica encapsulation of SERS labels, in which MPTMS makes the nanoparticle vitreophilic.[8] SERS signals of the Raman label (4-MBA) were normalized to the Raman band of ethanol at 882 cm^{-1}. For the complete monolayer coverage, the SERS signals were 22 ± 5 ($n = 3$ measurements) times more intense than those of the submonolayer coverage (Figure 5a). In addition to the maximum surface coverage with approximately 45 000 Raman

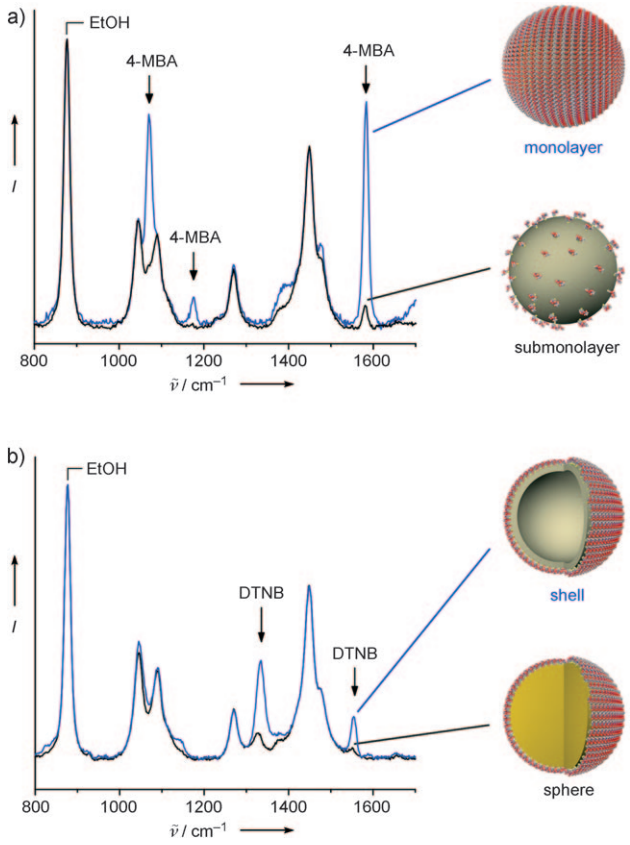

Figure 5. a) Influence of the surface coverage on the SERS signal strength: complete SAM compared to submonolayer coverage with Raman labels. b) Influence of the SERS substrate: Au/Ag nanoshells compared with Au nanospheres for red laser excitation.[16]

labels,[15] also the efficiency of the SERS substrate upon red laser excitation must be considered (see the Supporting Information).[11b] The comparison between gold/silver nanoshells and gold nanospheres as SERS substrates is shown in Figure 5b. In both cases the same Raman label precursor, 5,5′-dithiobis(2-nitrobenzoic acid), was used. 60 nm gold/silver nanoshells exhibit 4.6 ± 0.7 ($n = 4$) times more intense signals than gold nanospheres of the same size. Both colloidal solutions were filtered with 220 nm and 100 nm filters to remove dimers and then measured at same optical densities. According to Mie calculations, the extinction coefficient of the 60 nm gold/silver nanoshells is 1.7 times larger than that of the gold nanospheres (see the Supporting Information). This is equivalent to a roughly eightfold increase in sensitivity for the same particle concentration. Together, the two parameters—surface coverage (SAM vs. submonolayer) and SERS efficiency of the substrate (Au/Ag shell vs. Au sphere)—result in an increase in overall brightness by a factor of $\approx 176 = 22 \times 8$ compared with existing SERS labels based on single gold nanospheres with submonolayer coverage.[8]

The improved SERS labels were tested for tissue imaging, using prostate-specific antigen (PSA) as the target protein. The corresponding immuno-SERS labels contain approximately 225 antibody copies per nanoparticle (see the Supporting Information). SERS microscopic experiments with red laser excitation clearly demonstrate the specific binding of SERS-labeled PSA antibodies in the epithelium of the prostate combined with high signal levels and minimal autofluorescence (see the Supporting Information).

Experimental Section

Silver nitrate, polyvinylpyrrolidone (PVP), ethylene glycol, tetrachloroauric(III) acid ($HAuCl_4$), 5,5′-dithiobis(2-nitrobenzoic acid) (DTNB), 4-mercaptobenzoic acid (4-MBA), poly(allylamine hydrochloride) (PAH), tetraethoxyorthosilicate (TEOS), 3-amino-*n*-propyltrimethoxysilane (APTMS), 3-mercapto-*n*-propyltrimethoxysilane (MPTMS), 2-propanol, ethanol, and phosphate-buffered saline (PBS) were purchased from Sigma/Aldrich/Fluka. Succinimidyl-[(*N*-maleimidopropionamido)(dodecaethylenglycol)] ester (heterobifunctional cross-linker) was purchased from Pierce Biotechnology. Monoclonal mouse antihuman prostate-specific antigen (PSA) was obtained from Dako cytomation. In all reaction steps ultrapure water (18.2 MΩ) was used.

Silica encapsulation of SAM-coated SERS labels: The synthesis of SERS labels is described in the Supporting Information. The colloidal SERS label solution was centrifuged twice (40 min, 4000 rpm) to remove excess Raman label molecules and then redispersed in water. This solution was added dropwise with vigorous stirring to an aqueous solution of PAH (2 g L^{-1} PAH and 3.5 g L^{-1} NaCl in water), which had been sonicated for 15 min. The solution was stirred for 3 h and then centrifuged for 40 min at 4000 rpm. The gold/silver colloid was redispersed in H_2O and added dropwise to an aqueous PVP solution (4 g L^{-1} PVP in H_2O). The solution was then stirred and allowed to react overnight. The solution of polyelectrolyte-coated particles was centrifuged twice at 4000 rpm for 40 min and redispersed in a mixture of water and 2-propanol. A mixture of ammonia and 2-propanol (4 vol% NH_3) was added. TEOS (1 vol% TEOS in 2-propanol) was added with vigorous stirring in six portions over 6 h. The thickness of the silica shell can be changed by adjusting the amount of TEOS. A similar procedure was used for the silica encapsulation of cetyltrimethylammonium bromide (CTAB)-stabilized gold nanorods.[17] The morphology and the shell thickness of the

silica-coated SERS labels were determined by transmission electron microscopy (Figure 2).

Received: September 13, 2008
Published online: February 4, 2009

Keywords: labeling · nanotechnology · Raman spectroscopy · SERS microscopy · tissue diagnostics

[1] a) *Nanobiotechnology* (Eds.: C. M. Niemeyer, C. A. Mirkin), Wiley-VCH, Weinheim, **2004**; b) *Nanobiotechnology II* (Eds.: C. A. Mirkin, C. M. Niemeyer), Wiley-VCH, Weinheim, **2007**.

[2] a) *New Frontiers in Ultrasensitive Bioanalysis* (Ed.: X.-H. N. Xu), Wiley, New York, **2007**; b) *Nanomaterials for Cancer Diagnosis* (Ed.: C. Kumar), Wiley-VCH, Weinheim, **2007**; c) *Nanomaterials for Medical Diagnosis and Therapy* (Ed.: C. Kumar), Wiley-VCH, Weinheim, **2007**.

[3] a) R. Aroca, *Surface-Enhanced Vibrational Spectroscopy*, Wiley, New York, **2006**; b) K. A. Willets, R. P. Van Duyne, *Annu. Rev. Phys. Chem.* **2007**, *58*, 267 – 297; c) D. A. Stuart, A. J. Haes, C. R. Yonzon, E. M. Hicks, R. P. Van Duyne, *IEE Proc. Nanobiotechnol.* **2005**, *152*, 13 – 32.

[4] a) Y. C. Cao, R. Jin, C. A. Mirkin, *Science* **2002**, *297*, 1536 – 1540; b) D. Graham, B. J. Mallinder, D. Whitcombe, N. D. Watson, W. E. Smith, *Anal. Chem.* **2002**, *74*, 1069 – 1074.

[5] a) D. Graham, B. J. Mallinder, W. E. Smith, *Angew. Chem.* **2000**, *112*, 1103 – 1105; *Angew. Chem. Int. Ed.* **2000**, *39*, 1061 – 1063; b) D. Graham, K. Faulds, W. E. Smith, *Chem. Commun.* **2006**, 4363 – 4371; c) K. Faulds, F. McKenzie, W. E. Smith, D. Graham, *Angew. Chem.* **2007**, *119*, 1861 – 1863; *Angew. Chem. Int. Ed.* **2007**, *46*, 1829 – 1831.

[6] a) J. Ni, R. J. Lipert, G. B. Dawson, M. D. Porter, *Anal. Chem.* **1999**, *71*, 4903 – 4908; b) D. S. Grubisha, R. J. Lipert, H.-Y. Park, J. Driskell, M. D. Porter, *Anal. Chem.* **2003**, *75*, 5936 – 5943; c) Y. C. Cao, R. Jin, J.-M. Nam, C. S. Thaxton, C. A. Mirkin, *J. Am. Chem. Soc.* **2003**, *125*, 14676 – 14677; d) X. Su, J. Zhang, L. Sun, T.-W. Koo, S. Chan, N. Sundararajan, M. Yamakawa, A. A. Berlin, *Nano Lett.* **2005**, *5*, 49 – 54; e) J.-H. Kim, J.-S. Kim, H. Choi, S.-M. Lee, B.-H. Jun, K.-N. Yu, E. Kuk, Y.-K. Kim, D. H. Jeong, M.-H. Cho, Y.-S. Lee, *Anal. Chem.* **2006**, *78*, 6967 – 6973.

[7] a) D. Graham, B. J. Mallinder, W. E. Smith, *Biopolymers* **2000**, *57*, 85 – 91; b) Y. C. Cao, R. Jin, C. A. Mirkin, *Science* **2002**, *297*, 1536 – 1540; c) R. Jin, Y. C. Cao, C. S. Thaxton, C. A. Mirkin, *Small* **2006**, *2*, 375 – 380.

[8] a) S. P. Mulvaney, M. D. Musick, C. D. Keating, M. J. Natan, *Langmuir* **2003**, *19*, 4784 – 4790; b) W. E. Doering, S. Nie, *Anal. Chem.* **2003**, *75*, 6171 – 6176; c) W. E. Doering, M. E. Piotti, M. J. Natan, R. G. Freeman, *Adv. Mater.* **2007**, *19*, 3100 – 3108.

[9] a) S. Schlücker, B. Küstner, A. Punge, R. Bonfig, A. Marx, P. Ströbel, *J. Raman Spectrosc.* **2006**, *37*, 719 – 721; b) L. Sun, K.-B. Sung, C. Dentinger, B. Lutz, L. Nguyen, J. Zhang, H. Qin, M. Yamakawa, M. Cao, Y. Lu, A. J. Chmura, J. Zhu, X. Su, A. A. Berlin, S. Chan, B. Knudsen, *Nano Lett.* **2007**, *7*, 351 – 356.

[10] a) Y. G. Sun, B. T. Mayers, Y. N. Xia, *Nano Lett.* **2002**, *2*, 481 – 485; b) Y. Sun, Y. Xia, *Anal. Chem.* **2002**, *74*, 5297 – 5305.

[11] a) J. B. Jackson, N. J. Halas, *Proc. Natl. Acad. Sci. USA* **2004**, *101*, 17930 – 17935; b) M. Gellner, B. Küstner, S. Schlücker, *Vib. Spectrosc.* **2008**, DOI: 10.1016/j.vibspec.2008.07.011.

[12] a) X. Qian, X.-H. Peng, D. O. Ansari, Q. Yin-Goen, G. Z. Chen, D. M. Shin, L. Yang, A. N. Young, M. D. Wang, S. Nie, *Nat. Biotechnol.* **2008**, *26*, 83 – 90; b) S. Keren, C. Zavaleta, Z. Cheng, A. de la Zerda, O. Gheysens, S. S. Gambhir, *Proc. Natl. Acad. Sci. USA* **2008**, *105*, 5844 – 5849.

[13] G. T. Hermanson, *Bioconjugate Techniques*, Academic Press, San Diego, **2008**.

[14] W. Stöber, A. Fink, E. Bohn, *J. Colloid Interface Sci.* **1968**, *26*, 62 – 69.

[15] This number was calculated for particles 60 nm in diameter using data from an STM study on SAMs (0.26 nm^2 per molecule): A. H. Schäfer, C. Seidel, L. Chi, H. Fuchs, *Adv. Mater.* **1998**, *10*, 839 – 842.

[16] The concentration of the colloid with submonolayer coverage is twice that with monolayer coverage (a); the concentration of the Au nanospheres is 1.7 times greater than that of the Au/Ag nanoshells, while the optical density is the same (b).

[17] I. Pastoriza-Santos, J. Perez-Juste, L. M. Liz-Marzan, *Chem. Mater.* **2006**, *18*, 2465 – 2467.

